A Journal of the Gesellschaft Deutscher Chemiker

Angewandte International Edition

GDCh

Chemie

www.angewandte.org

Accepted Article

Title: Long-life room-temperature sodium-sulfur batteries by virtue of transition metal nanocluster-sulfur interactions

Authors: binwei zhang, tian sheng, yunxiao wang, shulei chou, Kenneth Davey, Shi-Xue Dou, and Shizhang Qiao

To be cited as: *Angew. Chem. Int. Ed.* 10.1002/anie.201811080
Angew. Chem. 10.1002/ange.201811080

Link to VoR: http://dx.doi.org/10.1002/anie.201811080
http://dx.doi.org/10.1002/ange.201811080

WILEY-VCH

10.1002/anie.201811080

WILEY-VCH

Long-life room-temperature sodium-sulfur batteries by virtue of transition metal nanocluster-sulfur interactions

Bin-Wei Zhang,[a, b]† Tian Sheng,[c]† Yun-Xiao Wang,[b] Shulei Chou,[b] Kenneth Davey,[a] Shi-Xue Dou[b] and Shi-Zhang Qiao*[a, d]*

Abstract: Room-temperature sodium-sulfur (RT-Na/S) batteries hold significant promise for large-scale application because of low cost of both sodium and sulfur. However, the dissolution of polysulfides into the electrolyte limits practical application. Here, we report the design and testing of a new class of sulfur hosts as transition metal (Fe, Cu, and Ni) nanoclusters (~ 1.2 nm) wreathed on hollow carbon nanospheres (S@M-HC) for RT-Na/S batteries. A chemical couple between the metal nanoclusters and sulfur is hypothesized to assist in immobilization of sulfur and to enhance conductivity and activity. S@Fe-HC exhibited an unprecedented reversible capacity of 394 mAh g^{-1} despite 1000 cycles at 100 mA g^{-1}, together with the a rate capability of 220 mAh g^{-1} at a high current density of 5 A g^{-1}. Importantly, density functional theory calculations underscore that these metal nanoclusters serve as electrocatalysts to rapidly reduce Na_2S_4 into short-chain sulfides and thereby obviate the 'shuttle effect'. We conclude these novel S host cathodes will provide new opportunities to construct electrode materials for various practical battery technologies.

Room-temperature sodium-sulfur (RT-Na/S) batteries have attracted significant attention due to the abundance, non-toxicity, low cost and high theoretical capacity of sulfur (1672 mAh g^{-1}). [1] However, RT-Na/S batteries present a practical challenge (widely known also to afflict Li-S batteries) of low reversible capacity and rapid capacity fade. [2] The low accessible capacity is caused by the insulating nature of sulfur and the sluggish reactivity of sulfur with sodium. This results in an incomplete reduction, rather than the complete production of Na_2S. [3] The dissolution of polysulfides into the electrolyte during cycling i.e. the 'shuttle effect', is the key reason for rapid capacity fade. [4]

Recently, significant gains have been made in attempting to solve these problems through novel S host materials, including hollow carbon spheres, [5] interconnected mesoporous carbon hollow nanospheres, [6] carbon fibre cloth, [7] and conducting polymer. [8] Although the carbon matrix used can improve performance of RT-Na/S batteries, their nonpolar character means they cannot effectively chemically interact with polar sodium polysulfides. This results in capacity decay. An improved rational design of cathode materials to inhibit polysulfides dissolution is therefore urgently required for RT-Na/S batteries.

S hosts, with inherent polarization, are expected to enhance reactivity of S and impede the shuttle effect. [9] These S host cathodes with intrinsic sulfiphilic properties, such as metal sulfides [9] and metal oxides [10], bind polysulfides and prevent their dissolution into the electrolyte. These however have been limited to TiO_2, [11] Cu/CuS_x, [12] Cu current foam [13] and SSe [14] for construction of intrinsic sulfiphilic hosts in RT-Na/S batteries. Moreover, the interaction between the polar surface of S hosts with polysulfides is limited, and sodium polysulfides remain prone to dissolution into the electrolyte. Recently, a strategy was established to circumvent this through reduction of polysulfides into short-chain sulfides, and production of Na_2S. This reduction conversion can obviate dissolution of sodium polysulfides and achieve, simultaneously, an improved capacity. [15] Transition metal-based catalysts however have received significant attention because of low cost and abundance and, generally, excellent catalytic performance across a range of electrochemical reduction reactions. [16] It was hypothesized that the introduction of these metals into RT-Na/S batteries, to reduce polysulfides to short-chain sulfides, might lower the decomposition energy barrier of polysulfides. Additionally, that transition metals such as Fe, Cu and Ni, would form a chemical bond with S and significantly improve conductivity of an S cathode. [14, 17]

Here, we report transition metal (M = Fe, Cu, and Ni) nanoclusters loaded onto hollow carbon nanospheres (HC) as new, polarized S hosts to improve the reactivity of S and to inhibit the shuttle effect. These transition metal nanoclusters enhance reactivity of S via chemical coupling. We show, perhaps surprisingly, that the Fe nanocluster (~1.2 nm) wreathed S host, S@Fe-HC, exhibits the greatest reversible capacity of initially 1023 mAh g^{-1}, and 394 mAh g^{-1} despite 1000 cycles at 100 mA g^{-1}. The role of these transition metal nanoclusters in RT-Na/S batteries is explored using density functional theory (DFT) calculations to underscore that metal nanoclusters serve as electrocatalysts and reduce long-chain polysulfides to short-chain sulfides and thereby prevent the shuttle effect.

Transmission electron microscope (TEM) images of HC revealed that these are homogeneous with a thickness of 5.1 nm (see Figure S1 in the Supporting Information). Metal (M = Fe, Cu, and Ni) nanoclusters supported on HC (denoted as M-HC) were successfully fabricated through controlled thermal treatment. TEM images of M-HC demonstrated that the metal nanoclusters had a uniform distribution, in which the average diameter was 1.1 nm (Figure S2-S4). Melted sulfur was loaded into the M-HC through a facile melt-diffusion strategy at 155 °C

[a] Mr. Bin-Wei Zhang, Dr. Kenneth Davey, Prof. Shi-Zhang Qiao
School of Chemical Engineering, The University of Adelaide, Adelaide, South Australia 5005, Australia
E-mail: s.qiao@adelaide.edu.au
[b] Mr. Bin-Wei Zhang, Dr. Yun-Xiao Wang, Dr. Shulei Chou, Prof. Shi-Xue Dou
Institute for Superconducting and Electronic Materials, Australian Institute of Innovative Materials, University of Wollongong, Innovation Campus, Squires Way, North Wollongong, New South Wales 2500, Australia
E-mail: yunxiao@uow.edu.au
[c] Prof. Tian Sheng
College of Chemistry and Materials Science, Anhui Normal University, Wuhu, 241000, P. R. China
[d] Prof. Shi-Zhang Qiao
School of Materials Science and Engineering, Tianjin University, Tianjin 300072, P.R. China
† These authors contributed equally to this work.

Supporting information for this article is given via a link at the end of the document.

for 12 h, then sealed in a quartz ampoule and kept at 200 °C for 2 h (S@M-HC). Atomic resolution, high-angle annular dark field (HAADF) scanning transmission electron microscope (STEM) images of S@Fe-HC demonstrated that the Fe-HC matrix all but completely kept its morphology after S loading without any aggregation on the HC of Fe nanoparticles and S (Figure 1). As can be seen in Figure 1b and 1d, the Fe nanoclusters were amorphous and well-dispersed on the HC, with an average size of ~1.3 nm (Figure 1f). Interestingly, after loading S, the size of Fe nanoclusters in S@Fe-HC increased about ~0.2 nm compared with the Fe-HC matrix (Figure S2). This indicates that S is chemically adsorbed on the Fe nanoclusters to form Fe-S bonds. The element mapping and line-profile analysis of S@Fe-HC demonstrated that the S is well-embedded in the carbon shell and that the amorphous Fe nanoclusters are distributed on the carbon shell (Figure 1c and 1e). It should be noted that the intensity of S increases with increasing intensity of Fe, suggesting that the presence of Fe nanoclusters immobilize S by formation of Fe-S bonds. The HAADF-STEM images of S@Cu-HC and S@Ni-HC demonstrate that these share a similar structure with S@Fe-HC, where the average size of amorphous Cu and Ni nanoclusters are 1.3 ± 0.3 nm (Figure S6) and 1.2 ± 0.3 nm (Figure S7), respectively. This approximately similar size of the three cathode materials permits a reliable comparison of results. Significantly, the size of the M nanoclusters in S@Cu-HC and S@Ni-HC are meaningfully larger when compared to counterparts without S loading (Figure S2 and Figure S3). This indicates that these also form Cu-S and Ni-S bonds and that these chemical bonds between metal nanoclusters and S are able to chemically stabilize S and improve its conductivity. [15, 18]

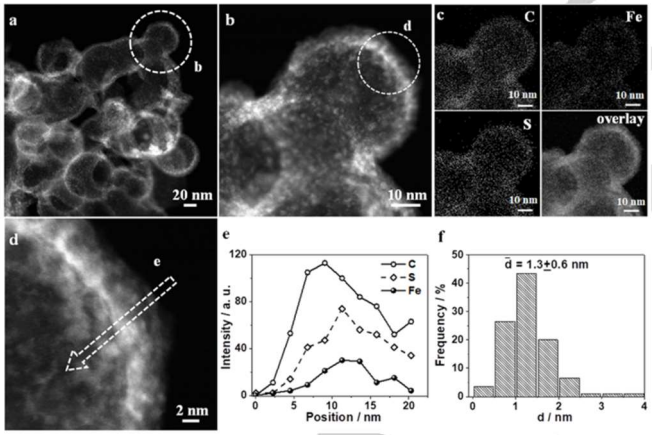

Figure 1 a-d, HAADF-STEM images and corresponding elemental mapping images of S@Fe-HC. **e,** Line-profile analysis as indicated in **d. f,** Histogram showing size distribution of Fe nanoclusters based on a count of 200 nanoclusters.

The thermogravimetric analysis (TGA) of these three samples indicates that the S content in S@Fe-HC, S@Cu-HC and S@Ni-HC are, respectively, ~ 40, 35, and 30 % (Figure 2a). The greatest S loading ratio with S@Fe-HC, shows that the amorphous Fe nanoclusters are favourable for capture of S and increases its loading. In particular, the amount of S in S@Fe-HC, measured through sublimation at high temperature (450 °C), is greatest at ~ 21%. This can be attributed to formation of the Fe-S bonds. This means also that the Fe-S bond is strongest amongst these M-S bonds. Inductively coupled plasma-optical emission spectroscopy (ICP-OES) results reveal that the Fe, Cu, and Ni content in S@Fe-HC, S@Cu-HC and S@Ni-HC are very similar, with weight ratios of, respectively, 9.82, 9.56 and 9.23, %. This approximately equal metal nanocluster loading makes for a reliable comparison of the results of TGA. X-ray diffraction (XRD) patterns of S@Fe-HC, S@Cu-HC, S@Ni-HC and S powder are shown as Figure 2b. The peaks in these four samples reveal that the S is crystalline. The lack of typical XRD peaks with Fe, Cu and Ni underscore the STEM results that these metal nanoclusters are amorphous. X-ray photoelectron spectroscopy (XPS) results are presented as Figure 2c, 2d and Figure S9 and S10. The Fe 2p XPS spectrum of S@Fe-HC could be separated into Fe^0 (707.10 eV) and Fe^{2+} (712.30 eV). The Fe^0 state in S@Fe-HC highlights the amorphous phase of the Fe nanoclusters. It is seen that the binding energy of Fe^0 $2p_{3/2}$ peak (707.1 eV) is right-shifted 0.1 eV compared with that for pure Fe (707.0 eV). This implies the formation of Fe-S bonds between Fe nanoclusters and S. To further prove this hypothesis, the S 2p spectrum is presented as Figure 2d. The S $2p_{3/2}$ peak of S@Fe-HC is at 163.90 eV, which is 0.10 eV left-shifted compared with pure S (S $2p_{3/2}$,164.0 eV). This shift can explain the enhancement of immobilization and reactivity of S through formation of the Fe-S bonds. Interestingly, this phenomenon was found also in S@Cu-HC and S@Ni-HC. The binding energies of the Cu^0 $2p_{3/2}$ XPS peak and the Ni^0 $2p_{3/2}$ XPS are 932.8 eV and 852.8 eV, which both are right-shifted by 0.1 eV from those of pure Cu (932.7 eV) and pure Ni (852.7 eV), whilst the S $2p_{3/2}$ peaks of S@Cu-HC and S@Ni-HC are both at 163.90 eV. This implies that Cu nanoclusters and Ni nanoclusters also form Cu-S and Ni-S bonds.

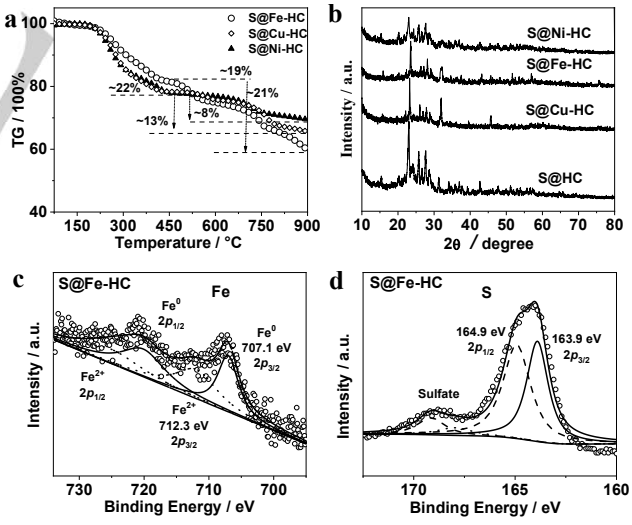

Figure 2 a, Thermogravimetry of S@Fe-HC, S@Cu-HC and S@Fe-HC. **b,** XRD patterns of S@Fe-HC, S@Cu-HC, S@Ni-HC, and S@HC. **c,** S 2*p* and **d,** Fe 2*p* XPS spectra for S@Fe-HC.

Cyclic voltammetry (CV) was measured to investigate the sodiation/desodiation mechanism of S@M-HC (Figure 3a and Figure S12). The S@Fe-HC cell presented four conspicuous peaks at 1.92, 1.54, 1.40, and 0.8, V during the initial cathodic scan. The greatest peak at 1.92 V corresponds to the transformation of solid sulfur into dissolved liquid long-chain

polysulfides (Na_2S_x, $4 < x \leq 8$), whilst the second peak at 1.54 V is attributed to added sodiation of Na_2S_x to Na_2S_4. The peak at 1.40 V, Na_2S_4 implies further sodiation to short-chain sulfides (Na_2S_y, $1 < y \leq 3$) and the peak at 0.8 V corresponds to the final Na_2S product. These four pairs of peaks were highly reproducible, suggesting good cycling stability of S@Fe-HC. Interestingly, the greater-voltage peaks of S@Cu-HC (1.93 V) and S@Ni-HC (1.94 V) are greater than that for S@Fe-HC (Figure S12). This indicates for S@Fe-HC that the highest energy is that dissociated from the Fe-S bonds. [17] This finding suggests also that the chemical bond between Fe and S is strongest, and results in better electrochemical performance of S@Fe-HC. The discharge/charge profiles of the 1st, 2nd, and 3rd cycles at 100 mA g^{-1} of S@Fe-HC, S@Cu-HC and S@Ni-HC cathode materials are shown in Figure 3b and Figure S15. The RT-Na/S@Fe-HC cell shows two, long plateaus during the first discharge from 1.75 to 1.18 V, and from 1.18 to 0.8, V. This high-voltage plateau is attributed to the transition from S to long-chain polysulfides Na_2S_x, whilst the low-voltage plateau is attributed to the reduction of Na_2S_x to short-chain sulfides Na_2S_y. The plateaus for S@Fe-HC are less well-defined than those for S/Fe-HC (Figure S16), S@Cu-HC and S@Ni-HC. This less defined plateau for S@Fe-HC likely originates from two main causes. The first is the strong chemical bond formed by S and Fe. This bond will affect the reaction of sulfur with sodium i.e. additional energy is needed to dissociate sulfur, and results in the plateau being less defined than that for S/Fe-HC. [18] The second is that Fe nanoclusters serve as electrocatalysts to rapidly reduce long-chain polysulfides into short-chain sulfides, which results in the low-voltage plateau not apparent. The long cycling-stabilities of S@Fe-HC, S@Cu-HC and S@Ni-HC cathodes are shown over 1000 cycles at 0.1 A g^{-1} (Figure 3c). The S@Fe-HC delivered an initial capacity of 1023 mAh g^{-1}, and an excellent reversible capacity of 394 mAh g^{-1} after 1000 cycles. In contrast, the S@Cu-HC and S@Ni-HC cathodes delivered initial capacities of 945 mAh g^{-1} and 783 mAh g^{-1}, respectively, and following > 1000 cycles, maintained 263 mAhg^{-1} and 201 mAh g^{-1}. It should be noted that these cathode materials displayed clear capacity decay over the first 50 cycles, due to dissolution of long-chain polysulfides from the outer carbon-shell. These cells all presented relatively stable cycling for the following 1000 cycles. S@Fe-HC maintained the greatest cycling stability. This likely originates from the ability of the amorphous Fe nanoclusters to enhance reactivity of S by formation of Fe-S bonds and impede dissolution of remaining long-chain polysulfides. Significantly, S/Fe-HC displays rapid capacity degradation. From an initial reversible capacity of 811 mA h g^{-1} it degraded to 57 mA h g^{-1} after only 25 cycles. This rapid degradation of S/Fe-HC is due to the fact that the surface of S does not chemical couple with Fe nanoclusters that can quickly dissolve into the electrolyte. The rate-capacity tests of S@M-HC were carried out at different current densities (Figure 3d). As is seen, when compared with S@Cu-HC and S@Ni-HC, S@Fe-HC exhibited the greatest reversible capacity of ~ 820, 498, 383, 313, 269, and 220 mAh g^{-1}, at 0.1, 0.2, 0.5, 1, 2 and 5 A g^{-1}, respectively. Strikingly, when the current density was returned to 0.1 A g^{-1}, the capacity of RT-Na/S@Fe-HC was 534 mAh g^{-1}, whilst that for S@Cu-HC was 370 mAh g^{-1} and that for S@Ni-HC was 266 mAh g^{-1}. The likely reason for these clear differences in electrochemical performance was investigated during the initial charge-discharge process by electrochemical impedance spectra (EIS) (Figure 3e) that corresponds to the fitted lines of Nyquist plots. The equivalent circuit (inset in Figure 3e) consists of the electrolyte resistance (R_s), interfacial nanolayer resistance (R_{suf}), charge transfer resistance (R_{ct}), and Warburg impedance (W_o). R_{suf} is associated with the SEI film and R_{ct} with the kinetic resistance of charge transfer through the electrode boundary. [20] The R_{ct} values for S@Fe-HC, S@Cu-HC and S@Ni-HC were 243.0, 276.2 and 434.9 Ω, suggesting that Fe nanoclusters enhance conductivity of S and decrease R_{ct}.

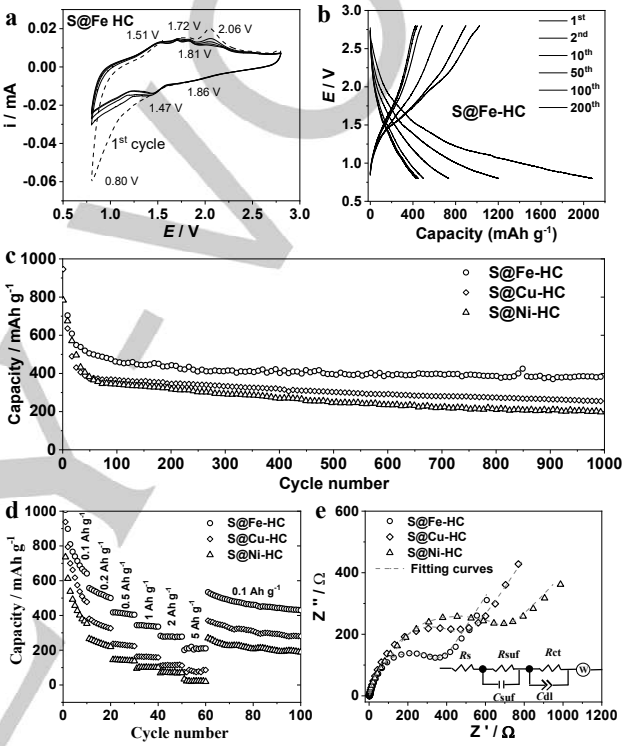

Figure 3. **a**, Cyclic voltammograms, and **b,** discharge/charge curves of S@Fe-HC at 100 mA g^{-1}. **c,** cycle performance, **d,** rate performance and **e,** Nyquist plots for S@Fe-HC, S@Cu-HC and S@Ni-HC (inset in **e:** the equivalent circuit model).

To investigate the role of M nanoclusters in realistic RT-Na/S batteries, ab initio molecular dynamics (AIMD) simulations [21] was preformed to reveal the decomposition of the Na_2S_4 following adsorption on Fe, Cu, and Ni nanoclusters/carbon. Figure 4a-c presents the structural evolution of Na_2S_4 and Na_2S_2, respectively, on metal nanoclusters as a function of AIMD simulation time. These results reveal that Na_2S_4 decomposes into Na_2S_2 on these nanoclusters. AIMD simulation results can be used to estimate the interaction between Na_2S_4 and metal nanoclusters and to gain understanding of the order of reactivity for these metal nanoclusters (Figure 4d**)**. The greater the reactivity of a nanocluster, the greater the adsorption energy of Na_2S_4 and the better performance in RT/Na-S batteries. The Fe nanocluster is the most active in reaction with Na_2S_4, which decomposed into Na_2S_2 in only 1 ps of the MD simulation. The dissociative adsorption energy converged to -10.24 eV. For the Cu nanocluster, after ~1 ps of MD simulation, the system

stabilized where the adsorption energy was -7.76 eV. The Na_2S_4 decomposition on the Ni nanocluster was found to be significantly slower than for the Fe and Cu nanoclusters. After ~ 2.3 ps of MD simulation, the total energy converged to give a value of the adsorption energy of -7.74 eV. It was observed that Na_2S_4 decomposed most rapidly on the Fe nanocluster. This observation highlights that the Fe nanocluster possessed the most suitable reactivity for RT/Na-S batteries.

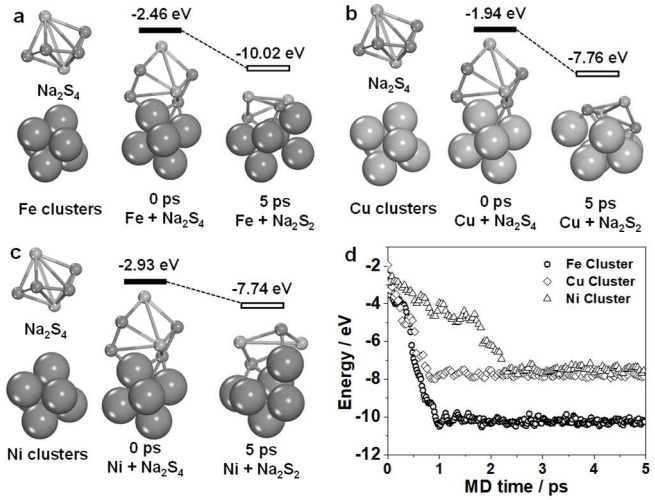

Figure 4 a-c, Na_2S_4 on Fe_6, Cu_6, and Ni_6 nanoclusters in the initial state at 0 ps, and at 5 ps. **d**, adsorption energies (eV) of Na_2S_4 on metal nanoclusters as a function of ab initio molecular dynamics simulation time (fs).

The ability of these three cathode materials to chemically adsorb polysulfides was evaluated by exposing Na_2S_4 to S@Fe-HC, S@Cu-HC and S@Ni-HC (Figure S17). The Na_2S_4 solution exhibited a peak for S_4^{2-} at ~ 313 cm^{-1}. [22] When the solution was exposed to S@Fe-HC this disappeared and another peak at ~ 252 cm^{-1} appeared. This finding is attributed to S_2^{2-}. [1a] For the solutions exposed to S@Cu-HC and S@Ni-HC the intensity of the S_4^{2-} peak decreased, and the S_2^{2-} peak evolved. This finding suggests that part of Na_2S_4 are converted to Na_2S_2. These findings indicated that S@Fe-HC gave the most efficient confinement of the polysulfides and electrocatalytically transformed these into short-chain sulfides – a finding consistent with corresponding DFT results. The electrochemical performance of the Fe/HC plain matrix is presented in Figures S18 and S19 in which the capacity contribution can be seen to be negligible for S@Fe-HC. Schematic illustrations of the M nanocluster electrode mechanism are presented as Figure S20. These M nanoclusters enhance the reactivity of S by formation M-S chemical bonds and bind polysulfide dissolution, and then catalyzed into short-chain sulfides.

In conclusion, we have designed and tested a new class of sulfur hosts as three transition metal (Fe, Cu, and Ni) nanoclusters (~ 1.2 nm) wreathed on hollow carbon nanospheres for RT-Na/S batteries, and hypothesized a chemical couple between the metal nanoclusters and sulfur that assists in immobilization of sulfur and enhances conductivity and activity. Of these, S@Fe-HC was found to exhibit an unprecedented reversible capacity of 394 mAh g^{-1} despite 1000 cycles at 100 mA g^{-1}, together with a rate capability of 220 mAh g^{-1} at a high current density of 5 A g^{-1}. Our new findings show that these metal nanoclusters serve as electrocatalysts to rapidly reduce Na_2S_4 into short-chain sulfides and thereby obviate the shuttle effect. These novel S host cathodes should prove to be of practical benefit in the construction of electrode materials for a range of battery technologies.

Acknowledgements

This research was supported by the Australian Research Council (ARC) (FL170100154, DP160104866, DP170104464 and DE170100928), the Commonwealth of Australia, through the Automotive Australia 2020 Cooperative Research Centre (Auto CRC).

Keywords: Metal nanoclusters • novel S hosts • electrocatalysts• shuttle effect• room temperature Na/S batteries

[1] a) S. Wei, S. Xu, A. Agrawral, S. Choudhury, Y. Lu, Z. Tu, L. Ma, L. A. Archer, *Nat. Commun.* **2016**, *7*, 11722; b) Xin, Y. X. Yin, Y. G. Guo, L. J. Wan, *Adv. Mater.* **2014**, *26*, 1261; c) J. Wang, J. Yang, Y. Nuli, R. Holze, *Electrochem. Commun.* **2007**, *9*, 31.

[2] a) P. Li, L. Ma, T. Wu, H. Ye, J. Zhou, F. Zhao, N. Han, Y. Wang, Y. Wu, Y. Li, J. Lu, *Adv. Energy Mater.* **2018**, *8*, 1800624; b) X. Xu, D. Zhou, X. Qin, K. Lin, F. Kang, B. Li, D. Shanmukaraj, T. Rojo, M. Armand, G. Wang, *Nat. Commun.* 2018, 9, 3870; c) X. Yu, A. Manthiram, *Chem. Mater.* **2016**, *28*, 896.

[3] Z. Qiang, Y. M. Chen, Y. Xia, W. Liang, Y. Zhu, B. D. Vogt, *Nano Energy* **2017**, *32*, 59;

[4] X. Yu, A. Manthiram, *J. Phys. Chem. Lett.* **2014**, *5*, 1943-1947.

[5] D. J. Lee, J. W. Park, I. Hasa, Y. K. Sun, B. Scrosati, J. Hassoun, *J. Mater. Chem. A* **2013**, *1*, 5256.

[6] Y. X. Wang, J. Yang, W. Lai, S. L. Chou, Q. F. Gu, H. K. Liu, D. Zhao, S. X. Dou, *J. Am. Chem. Soc.* **2016**, *138*, 16576.

[7] Q. Lu, X. Wang, J. Cao, C. Chen, K. Chen, Z. Zhao, Z. Niu, J. Chen, *Energy Storage Materials* **2017**, *8*, 77.

[8] S. Wei, L. Ma, K. E. Hendrickson, Z. Tu, L. A. Archer, *J. Am. Chem. Soc.* **2015**, *137*, 12143.

[9] G. Zhou, H. Tian, Y. Jin, X. Tao, B. Liu, R. Zhang, Z. W. Seh, D. Zhuo, Y. Liu, J. Sun, J. Zhao, C. Zu, D. S. Wu, Q. Zhang, Y. Cui, *Proc. Natl. Acad. Sci. USA* **2017**, *114*, 840.

[10] Q. Pang, D. Kundu, M. Cuisinier, L. F. Nazar, *Nat. commun.* **2014**, *5*, 4759

[11] D. Ma, Y. Li, J. Yang, H. Mi, S. Luo, L. Deng, C. Yan, M. Rauf, P. Zhang, X. Sun, X. Ren, J. Li, H. Zhang, *Adv. Funct. Mater.* **2018**, *28*, 1705537.

[12] S. Zheng, P. Han, Z. Han, P. Li, H. Zhang, J. Yang, *Adv. Energy Mater.* **2014**, *4*, 1400226.

[13] B. W. Zhang, Y. D. Liu, Y. X. Wang, L. Zhang, M. Z. Chen, W. H. Lai, S. L. Chou, H. K. Liu, S. X. Dou, *ACS Appl. Mater. Interfaces* **2017**, *9*, 24446.

[14] Y. Yao, L. Zeng, S. Hu, Y. Jiang, B. Yuan, Y. Yu, *Small* **2017**, *13*, 1603513.

[15] B. W. Zhang, T. Sheng, Y. D. Liu, Y. X. Wang, L. Zhang, W. H. Lai, L. Wang, J. Yang, Q. F. Gu, S. L. Chou, H. K. Liu, S. X. Dou, *Nat. Commun.* **2018**, *9*, 4082.

[16] a) G. Wu, K. L. More, C. M. Johnston, P. Zelenay, *Science* **2011**, *332*, 443; b) H. Jin, C. Guo, X. Liu, J. Liu, A. Vasileff, Y. Jiao, Y. Zheng, S. Z. Qiao, *Chem. Rev.* **2018**, *118*, 6337.

[17] Q. Zhao, X. F. Hu, K. Zhang, N. Zhang, Y. X. Hu, J. Chen, *Nano Lett.* **2015**, 15, 721.

[18] a) B. Zhang, X. Qin, G. R. Li, X. P. Gao, *Energy Environ. Sci.* **2010**, *3*, 1531; b) J. Wang, J. Yang, C. Wan, K. Du, J. Xie, N. Xu, *Adv. Funct. Mater.* **2003**, *13*, 487.

[19] T. H. Hwang, D. S. Jung, J. S. Kim, B. G. Kim, J. W. Choi, *Nano Lett.* **2013**, *13*, 4532.

[20] G. Tan, R. Xu, Z. Xing, Y. Yuan, J. Lu, J. Wen, C. Liu, L. Ma, C. Zhan, Q. Liu, T. Wu, Z. Jian, R. Shahbazian-Yassar, Y. Ren, D. J. Miller, L. A. Curtiss, X. Ji, K. Amine, *Nat. Energy* **2017**, *2*, 17090.

[21] a) G. Kresse, J. Hafner, *Phy. Rev. B* **1994**, *49*, 14251; b) G. Kresse, J. Furthmuller, *Comput. Mater. Sci.* **1996**, *6*, 15.

[22] H. Al Salem, V. R. Chitturi, G. Babu, J. A. Santana, D. Gopalakrishnan, L. M. Reddy Arava, *RSC Adv.* **2016**, *6*, 110301.

10.1002/anie.201811080

WILEY-VCH

COMMUNICATION

Transition metal nanoclusters (~1.2 nm) wreathed on hollow carbon nanospheres as novel S hosts were applied to enhance conductivity and activity of sulfur. These nanoclusters chemisorb the resultant polysulfide and electro-catalyze these into short-chain sulphides, to achieve excellent cycling stability and rate performance for room-temperature sodium sulfur batteries.

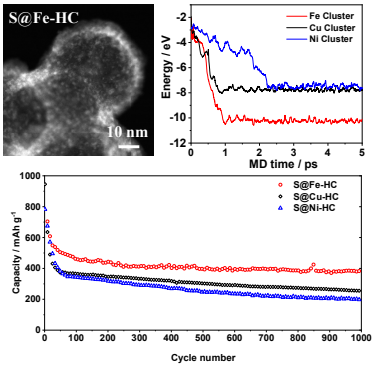

Bin-Wei Zhang, Tian Sheng, Yun-Xiao Wang, Shulei Chou, Kenneth Davey, Shi-Xue Dou and Shi-Zhang Qiao**

Page No. – Page No.

Long-life room-temperature sodium-sulfur batteries by virtue of transition metal nanocluster-sulfur interactions